COMPRESSIBLE TURBULENT BOUNDARY-LAYER FLOW CONTROL OVER A WEDGE

M. Xenos[*1], **E. Tzirtzilakis**[2] and **N. Kafoussias**[2]

[1] University of Illinois at Chicago, Departments of Chemical Engineering and Bioengineering.
[2] University of Patras, Department of Mathematics, Division of Applied Analysis.

[*]e-mail: xenos@uic.edu

Keywords: compressible flow, turbulent boundary-layer, suction/injection, flow over a wedge

Abstract.

The effects of blowing and suction on the steady compressible boundary-layer flow with adverse pressure gradient and heat transfer over a wedge are numerically examined. The fluid is considered to be a compressible, viscous and Newtonian ideal gas (air) and it is subjected to a constant velocity of suction/injection applied globally to the wedge or locally to specific slots on the surface.

The Reynolds-Averaged Boundary-Layer (RABL) equations and their boundary conditions are transformed using the compressible Falkner-Skan transformation. The resulting coupled and nonlinear system of PDEs is solved using the Keller box method. For the eddy-kinematic viscosity the turbulent models of Cebeci-Smith and Baldwin-Lomax are employed. For the turbulent Prandtl number the extended model of Kays-Crawford is used.

Numerical calculations are carried out for the case of an adiabatic, cooled or heated wall and for different values of the dimensionless pressure-gradient parameter (m). The obtained results show that the flow field can be controlled by the suction/injection velocity for different values of the parameter m.

1 INTRODUCTION

A common area of interest in the field of aerodynamics is the investigation of compressible two-dimensional steady turbulent flows. One of the characteristic flow configuration, which is of fundamental importance, is that of the flow over a wedge. This type of flow constitutes a general class of problems in fluid mechanics in which the free stream velocity is proportional to a power of the length co-ordinate measured from the stagnation point.

The wedge flow investigated for the first time in 1931 by Falkner and Skan [1] which considered two-dimensional incompressible wedge flow. The incompressible laminar heat transfer of wedge flow was studied in [2] using a differential transformation method, whereas, the transient heat transfer boundary layer flow on a wedge with sudden change of thermal boundary conditions of uniform wall temperature and heat flux was investigated in [3]. The effect of the variable viscosity on the Falkner-Skan flow with constant wall temperature was investigated in [4]. The laminar compressible MHD flow over a wedge with suction or injection has been investigated in [5].

As far as the aerodynamics is concerned, the suction/injection has very often been used as an active aerodynamic flow control technique to prevent transition from laminar to turbulent flow as well as turbulent flow separation [6]. The combined influence of localized injection and localized suction retains the boundary-layer flow, reducing skin friction [7], [8]. Many passive and active techniques have been developed for the prevention or delay of flow separation. Passive techniques are currently employed via blown flaps on the tip of the aircraft wings or leading edge extensions and strakes on the nose of the wings (slats) or via vortex generators on various points on the wings [9]. Another means of boundary-layer control is by heating or cooling the wall [10].

The numerical investigation of the two–dimensional turbulent boundary-layer compressible flow, over a finite smooth and permeable flat surface, with an adverse pressure gradient and heat and mass transfer, was studied in [11]. It was found that the continuous suction/injection applied on the wall modulates the flow field and the separation point. The MHD incompressible laminar boundary-layer flow over a wedge with suction or injection was studied in [12].

As far as it could be investigated, the compressible turbulent boundary-layer flow over a wedge, has not been yet investigated. Hence, the aim of this work is the investigation of the classical wedge flow problem from the aerodynamics point of view. Thus, in the present paper the compressible turbulent boundary-layer flow, over a permeable wedge, in the presence of an adverse pressure gradient is numerically studied. The effects of localized suction, applied to the region of the separation point, are also examined. The boundary-layer flow is considered turbulent and two turbulent models are employed, those of Cebeci- Smith (C-S) and Baldwin-Lomax (B-L).

From the analysis of the obtained results it is concluded that localized suction influences the flow field and the separation point, rendering the above application a flow control technique.

2 MATHEMATICAL FORMULATION

The steady two-dimensional compressible turbulent boundary-layer flow over a permeable wedge is considered. The wedge is submerged in a heat-conducting perfect and Newtonian fluid (air) flowing with velocity u_∞ towards the wedge (Figure 1). The fluid on the wedge is subjected to suction or blowing through the entire surface or locally from slots on various locations on the surface of the wedge whereas the temperature of the surface of the wedge is $T_w(x)$.

Under the above assumptions, the equations governing this type of flow are the Reynolds-Averaged Boundary-Layer (RABL) equations [10], [11]. Using the Bernoulli equation, the pressure term in the *x*-momentum equation can be substituted by
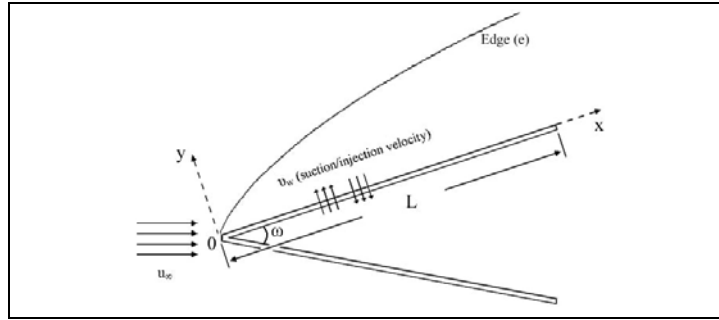

Figure 1. Flow configuration and coordinate system for the wedge.

$$-\frac{dp}{dx} = \rho_e u_e \frac{du_e}{dx}, \tag{1}$$

where the subscript *e* refers to the conditions at the edge of the boundary layer. In the flow over the wedge the velocity at the edge of the boundary layer can be written as [12]

$$u_e = u_\infty x^m, \quad m = \frac{\beta}{2-\beta} \geq 0, \tag{2}$$

where u_∞ is the free stream velocity and β is the Hartree pressure-gradient parameter that corresponds to $\beta = \omega/\pi$ for a total angle ω of the wedge. Using the abbreviation $\overline{\rho v}$ for $\rho v + \overline{\rho v}$ and omitting, for simplicity, the overbars on the basic time-average variables *u, v, ρ, p* and *T* the equations of the problem can now be written as in [11]:

$$\frac{\partial}{\partial x}(\rho u) + \frac{\partial}{\partial y}(\overline{\rho v}) = 0, \tag{3}$$

$$\rho u \frac{\partial u}{\partial x} + \overline{\rho v}\frac{\partial u}{\partial y} = \rho_e u_e \frac{du_e}{dx} + \frac{\partial}{\partial y}\left[\mu\frac{\partial u}{\partial y} - \rho\overline{u'v'}\right], \tag{4}$$

$$\rho u \frac{\partial H}{\partial x} + \overline{\rho v}\frac{\partial H}{\partial y} = \frac{\partial}{\partial y}\left[k\frac{\partial T}{\partial y} - c_p\rho\ \overline{T'v'} + u\left(\mu\frac{\partial u}{\partial y} - \rho\overline{u'v'}\right)\right]. \tag{5}$$

It is worth mentioning here that the total enthalpy *H* for a perfect gas is defined by the expression:

$$H = c_p T + \frac{1}{2}u^2 \tag{6}$$

Due to the parabolic nature of the above equations, boundary conditions must be provided on two sides of the solution domain in addition to the initial conditions at $x = x_0$. So, the boundary conditions of the problem under consideration are

$$y = 0 : u = 0, \ \upsilon = \upsilon_w(x), \ H = H_w(x) ,$$
$$y = \delta : u = u_e(x), \ H = H_e(x) . \tag{7}$$

In the above boundary conditions (7) δ is a distance sufficiently far away from the wall where the u velocity and total enthalpy H reach their free-stream values and $\upsilon_w(x)$ is the mass transfer velocity at the wall. In the case of an impermeable wall $\upsilon_w(x)$ is equal to zero, for the case of suction $\upsilon_w(x) < 0$ and for the case of injection $\upsilon_w(x) > 0$. Defining the eddy kinematic viscosity ε_m and turbulent Prandtl number Pr_t by the expressions

$$-\overline{u'\upsilon'} = \varepsilon_m \frac{\partial u}{\partial y}, \qquad -\overline{T'\upsilon'} = \frac{\varepsilon_m}{Pr_t} \frac{\partial T}{\partial y}, \tag{8}$$

the equations describing the problem can be written as

$$\frac{\partial}{\partial x}(\rho u) + \frac{\partial}{\partial y}(\overline{\rho \upsilon}) = 0, \tag{9}$$

$$\rho u \frac{\partial u}{\partial x} + \overline{\rho \upsilon} \frac{\partial u}{\partial y} = \rho_e u_e \frac{du_e}{dx} + \frac{\partial}{\partial y}\left[(\mu + \rho\varepsilon_m) \frac{\partial u}{\partial y} \right], \tag{10}$$

$$\rho u \frac{\partial H}{\partial x} + \overline{\rho \upsilon} \frac{\partial H}{\partial y} = \frac{\partial}{\partial y}\left\{ \left(\frac{\mu}{Pr} + \rho \frac{\varepsilon_m}{Pr_t} \right) \frac{\partial H}{\partial y} + \left[\mu\left(1 - \frac{1}{Pr} \right) + \rho\varepsilon_m\left(1 - \frac{1}{Pr_t} \right) \right] u \frac{\partial u}{\partial y} \right\}, \tag{11}$$

and the boundary conditions are

$$y = 0 : u = 0, \ \upsilon = \upsilon_w(x), \ H = H_w(x) ,$$
$$y = \delta : u = u_e(x), \ H = H_e(x) . \tag{12}$$

The above system of equations (9)-(12) consists by a coupled and nonlinear system of partial differential equations (PDEs). In order to solve the system of PDEs numerically, the compressible version of the Falkner-Skan transformation for a wedge is introduced, defined by

$$\eta(x,y) = \int_0^y \left(\frac{m+1}{2} \frac{u_e(x)}{\nu_e(x)\,x} \right)^{1/2} \frac{\rho(x,y)}{\rho_e(x)} dy, \quad \psi(x,y) = \left(\frac{2}{m+1} \rho_e\mu_e u_e x \right)^{1/2} f(x,\eta) \tag{13}$$

where $f(x,y)$ is the dimensionless stream function. Using the definition of the stream function ψ, for a compressible flow, that satisfies the continuity equation (9), with the relations

$$\rho u = \frac{\partial\psi}{\partial y}, \quad \overline{\rho\upsilon} = -\frac{\partial\psi}{\partial x} \tag{14}$$

and defining the dimensionless total energy ratio S as H/He, the system of the PDEs (9)-(12) becomes

$$(bf'')' + m_1 ff'' + m_2[c - (f')^2] = x\left[f' \frac{\partial f'}{\partial x} - f'' \frac{\partial f}{\partial x} \right], \tag{15}$$

$$(eS' + df'f'')' + m_1 f S' = x\left[f' \frac{\partial S}{\partial x} - S' \frac{\partial f}{\partial x} \right], \tag{16}$$

$$\eta = 0 : f' = 0, \ f_w(x) = f(x,0) = -\left(\frac{m+1}{2u_e\mu_e\rho_e x} \right)^{1/2} \int_0^x \rho_w(x,0)\upsilon_w(x)dx , \ S = S_w(x,0) ,$$
$$\eta = \eta_e : f' = 1, \ S = 1 , \tag{17}$$

where η_e is the dimensionless thickness of the boundary layer and primes denote partial differentiation with respect to η. The quantities $b, \ C, \ c, \ d, \ e, m_1, m_2$, etc. are defined as follows:

$$b = C\left(1 + \varepsilon_m^+ \right), \quad C = \frac{m+1}{2} \frac{\rho(x,\eta)\mu(x,\eta)}{\rho_e(x)\mu_e(x)} , \quad c = \frac{\rho_e(x)}{\rho(x,\eta)} ,$$
$$d = \frac{Cu_e^2(x)}{H_e(x)}\left[1 - \frac{1}{Pr} + \varepsilon_m^+\left(1 - \frac{1}{Pr_t} \right) \right] , \quad \varepsilon_m^+ = \frac{\varepsilon_m}{\nu(x,\eta)} , \tag{18}$$

$$e = \frac{C}{\Pr}\left(1 + \varepsilon_m^+ \frac{\Pr}{\Pr_t}\right), \quad m_2 = \frac{x}{u_e(x)}\frac{du_e(x)}{dx}, \quad R_x = \frac{u_e(x)x}{\nu_e(x)}$$

$$m_1 = \frac{1}{2}\left[1 + m_2 + \frac{x}{\rho_e(x)\mu_e(x)}\frac{d}{dx}(\rho_e\mu_e)\right].$$

Finally, the problem under consideration is described by the system of equations (15) and (16), subjected to the boundary conditions (17), whereas the coefficients entering into the equations are defined by the expressions (18).

3 TURBULENCE MODELS

In this study two algebraic turbulence models, Cebeci-Smith (C-S) and Baldwin-Lomax (B-L), are employed for the calculation of the eddy–viscosity ε_m and a model for the turbulent–Prandtl number $\Pr_t$. The C-S turbulent model [10], [13] is one of the simplest turbulence models and its accuracy has been explored for a wide range of experimental data. It is one of the "Zero–equation PDE models", using only PDEs for the mean velocity field, and no turbulence PDEs [15]. It has been used for a wide range of engineering problems giving sufficiently accurate results [11], [16]. The C-S turbulent model is a two-layer algebraic eddy viscosity model. According to the above, the turbulent boundary–layer is treated as a composite layer consisting of inner and outer regions with separate expressions for the eddy-kinematic viscosity in each region. For the inner region (viscous sublayer) the Prandtl–Van Driest formulation is used while for the outer region the Clauser formulation [10].

Baldwin and Lomax improved the C-S turbulent model avoiding the necessity for finding the edge of the boundary–layer. B-L is an algebraic turbulent model that also treats the turbulent boundary–layer as a composite layer consisting of inner and outer regions. For the inner region the Prandtl–Van Driest formulation is used. For the outer region, Baldwin and Lomax introduced a new formulation according to which the product $y_{MAX}F_{MAX}$ replaces $\delta^* u_e$ in the Clauser formulation of the Cebeci–Smith model and the combination $y_{MAX}U_{DIF}^2/F_{MAX}$ replaces δU_{DIF} in the wake formulation [17].

The Baldwin–Lomax turbulence model was developed for use in two, or three, dimensional Navier–Stokes machine codes [18], [19] and the results from it are in a good agreement with experimental data. Many researchers have adopted the Baldwin–Lomax algebraic model for its simplicity, although many modifications to its basic form have been employed [20]. In order to investigate the mass transfer through the plate, in the Baldwin–Lomax model of this study, a formula for the suction/injection velocity, it is adopted from the Cebeci–Smith model. So, the "damping–length" parameter A^+ is not considered as a constant taking the value 26, but as a function of the local density and viscosity values [10]. Finally for the turbulent–Prandtl number $\Pr_t$ a modification of the extended Kays and Crawford's model is used [8], [21].

4 NUMERICAL SOLUTION

The numerical scheme used to solve the parabolic system of PDEs (15)-(18) is a version of the Keller–box method [10], [11], [13], [22]. The scheme is unconditionally stable, and second–order accuracy is achieved with arbitrary x and η spacing [23]. The governing equations are written as a first–order system and derivatives of the unknown functions $f(x, \eta)$, $S(x, \eta)$ with respect to η are introduced as new functions. Using central–difference derivatives for the unknown functions at the midpoints of the net rectangle, the resulting difference equations are implicit and nonlinear. The box–differencing scheme with Newton linearization is then applied to the first–order PDEs, giving rise to a block tridiagonal system, which is solved by the block elimination method [24].

The derivative of the dimensionless heat-transfer parameter S_w' is considered to be equal to zero, $S_w' = 0$, describing no heat transfer between the plate and the fluid (adiabatic flow). For the heated/cooled of the wall the dimensionless heat-transfer parameter is considered $S_w > 1, (S_w = 2)$ and $S_w < 1, (S_w = 0.25)$. For determining the specific heat under constant pressure c_p, the Prandtl number Pr and the density ρ of the fluid (air) for temperatures varying from 100 to 2500 K, an interpolation formula is used. The data for the c_p, Pr and ρ were taken from tables [10], [25]. The values of each quantity, for every value of temperature, is calculated by the successive linear interpolation approach known as Neville's algorithm [26].

The code is proven to be grid independent and provides similar results for different grid realizations [27]. However, in this study a grid of 1001×81 points was used, where 81 points were used on the η-direction and 1001 on the x-direction.

For the numerical solution of the equations describing the problem the program is divided in two parts. The first is a dynamic link library (*DLL*) which contains all the algorithms for the numerical solution of the problem. The second part is a graphical user interface (*GUI*), where the user can review or alter the initial data, as, for

instance, the free stream Mach number, the temperature of the plate and the fluid, the suction/injection velocity, etc. The program was written in *FORTRAN 90* utilizing *OpenGL* for the visualization of the data [28].

5 RESULTS AND DISCUSSION

The results of this study concern dimensionless as well as dimensional quantities of the problem under consideration. It is very important to present results on the dimensionless local skin friction coefficient (Cf_x) and the local Stanton number (St_x) for the heated and cooled walls. It is also imperative to present results for dimensional quantities that will provide information for the shape of the compressible turbulent boundary layer under the adverse pressure gradient and the velocity and temperature fields throughout the boundary layer.

Figure 2a presents the velocity field on the upper wall of a wedge for $m = 0.05$ ($\beta = 17.2^{\circ}$). The boundary layer is always attached to the plate and never separates from the surface for Mach number $M_{\infty} = 1.0$. The figure also depicts the temperature field over the upper surface of the wedge for adiabatic wall (Figure 2b, $S'_w = 0$), heated (Figure 2c, $S_w = 2$) and cooled wall (Figure 2d, $S_w = 0.25$). The increase of temperature in the boundary layer for the adiabatic case is 18 degrees and this increase is due to viscous forces acting on the flow field and the inclination of the wall. The maximum temperature for the adiabatic case is 318 *K*, for the heated wall is 634 *K* and occurs near the heated wall. Finally, the maximum temperature for the cooled wall is 316 *K* and occurs near the edge of the boundary layer of the wedge as shown in Figure 2d.
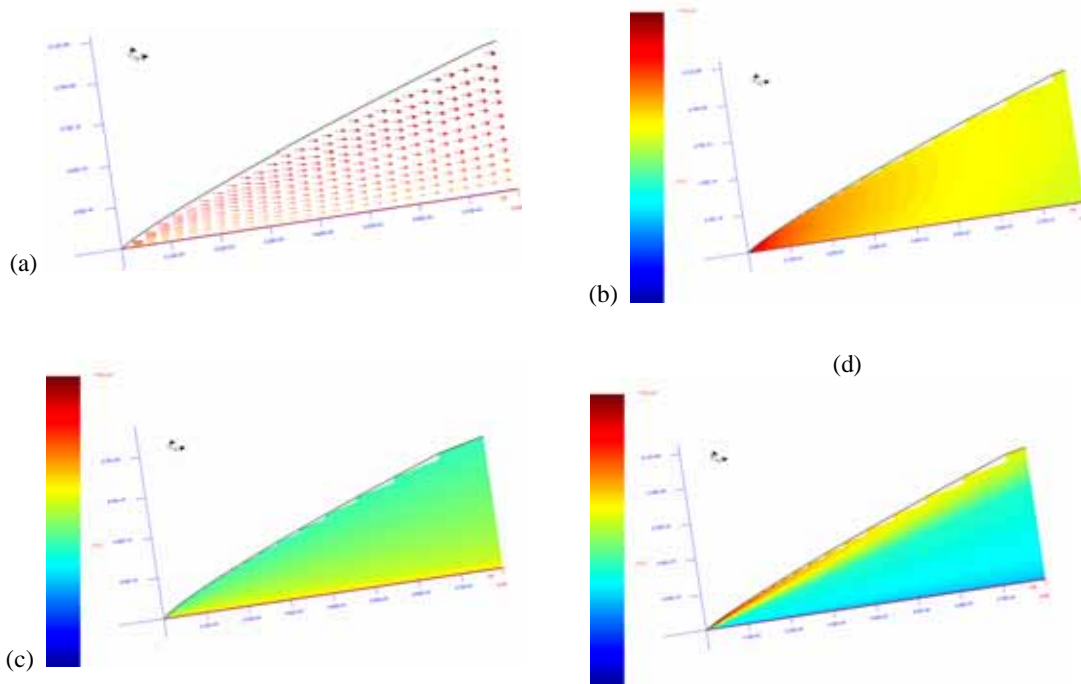

(a)

(b)

(d)

(c)

Figure 2. (a) Velocity field over a wedge, (b) Temperature field for an adiabatic wall, (c) Temperature field for a heated wall, (d) Temperature field for a cooled wall.

The flow over a flat plate at zero incidence, with constant external velocity, is known as Blasius flow and corresponds to the dimensionless pressure gradient $m = 0$. The dimensionless parameter m plays an important role in the problem under consideration because it denotes the shape factor of the velocity profiles [12]. It has been shown that when $m < 0$ (increasing pressure), the velocity profiles have a point of inflexion whereas when $m > 0$ (decreasing pressure), there is no point of inflexion for the laminar boundary layer [13]. In order to quantify the boundary layer over a wedge important dimensionless quantities, like the dimensionless local skin friction coefficient (Cf_x), the local Stanton number (St_x) and the total drag (D) over the wedge, are presented. Eq. (19) shows the relationship that connects these important quantities with the dimensionless shear parameter

on the wall $f_w'' = f''(x,0)$, the dimensionless heat transfer parameter $S_w' = S'(x,0)$ and the dimensionless total energy ratio $S_w = H_w/H_e$ on the wall of the wedge [11], [22].

$$Cf_x = \left(\frac{m+1}{2}\right)^{1/2} \frac{2C_w}{\sqrt{R_x}} f_w'', \qquad St_x = \left(\frac{m+1}{2}\right)^{1/2} \frac{C_w S_w'}{\Pr \sqrt{R_x} \left(1-S_w\right)}, \ \left(S_w \neq 1\right),$$

$$D = \left(\frac{m+1}{2}\right)^{1/2} \int_0^{x^*} \frac{C_w f_w''(x,0)}{\sqrt{\mathrm{Re}_x}} \rho_e(x) u_e^2(x)\, dx \tag{19}$$

where x^* is the distance of the separation point from the leading edge and $C_w = \rho_w \mu_w / \rho_e \mu_e$. Figure 3 shows the skin friction coefficient Cf_x against the distance x for various values of the parameter m, ($m = 0.0, 0.05, 0.095$), $M_\infty = 1.0$ and for the two turbulence models (C-S, B-L) for the case of an adiabatic wall. For larger values of the dimensionless parameter m ($m \geq 0.1$) the model predict instant separation of the turbulent compressible boundary layer. Both turbulent models give similar results and as the angle of the wedge is increased the total drag D and the skin friction coefficient Cf_x increase in both C-S and B-L models.
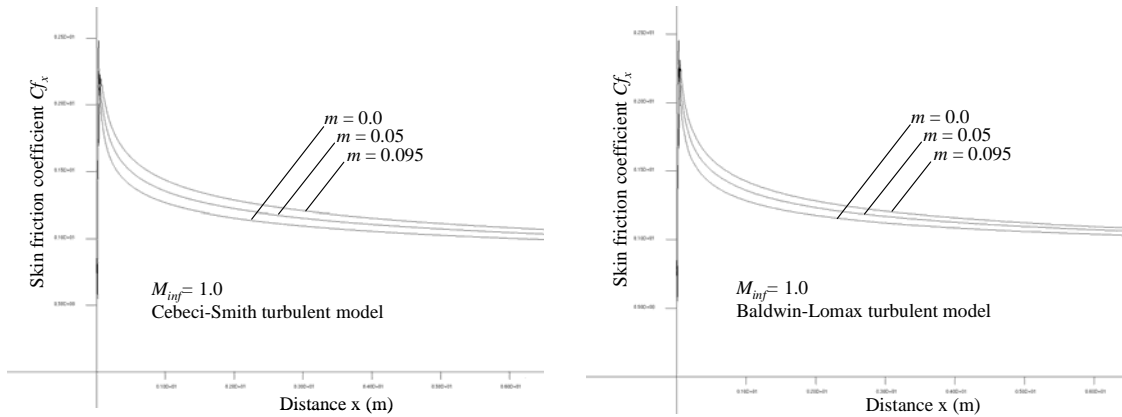

Figure 3. Skin friction coefficient Cf_x against the distance x for various values of the parameter m, $M_\infty = 1.0$ for the case of adiabatic wall (C-S - left, B-L - right).

The same behavior is shown for smaller ($M_\infty = 0.5$) or larger ($M_\infty = 1.5$) Mach numbers. The results for the total drag D for various Mach numbers M_∞, for both turbulent models and for $m = 0.0, 0.05, 0.095$ and for an adiabatic wall are summarized in Table 1.

	C-S model	B-L model
$M_\infty = 0.5$	$m = 0.0, D = 256.7$ $m = 0.05, D = 289.0$ $m = 0.095, D = 324.4$	$m = 0.0, D = 261.8$ $m = 0.05, D = 292.6$ $m = 0.095, D = 322.9$
$M_\infty = 1.0$	$m = 0.0, D = 886.3$ $m = 0.05, D = 949.8$ $m = 0.095, D = 994.4$	$m = 0.0, D = 910.7$ $m = 0.05, D = 967.0$ $m = 0.095, D = 1004.0$
$M_\infty = 1.5$	$m = 0.0, D = 1670.0$ $m = 0.05, D = 1718.3$ $m = 0.095, D = 1738.7$	$m = 0.0, D = 1701.0$ $m = 0.05, D = 1754.0$ $m = 0.095, D = 1798.6$

Table 1: Total drag D for various Mach numbers M_∞ and dimensionless pressure parameter m for adiabatic wall.

When the dimensionless pressure parameter m becomes 0.1 an instant separation of the compressible turbulent boundary layer occurs. One of the control methods that can retain the turbulent compressible boundary layer over the wedge for larger dimensionless pressure coefficients $m > 0.1$ is the application of continuous or localized suction/injection. Figure 4 shows the skin friction coefficient Cf_x against the distance x for $m = 0.095$

with no suction/injection and for $m = 0.1$ with the application of localized suction, near the tip of the wedge ($v_w(x) = -2.0 \times 10^{-4}$) and continuous suction at the whole length of the upper wall of the wedge ($v_w(x) = -1.0 \times 10^{-4}$). It is apparent that the boundary layer can be retained with the application of suction/injection, but the total drag D increases especially in the case of continuous suction/injection. Finally, in Figure 5 the local Stanton number (St_x) is presented for heated and cooled walls and different values of the dimensionless pressure parameter m.
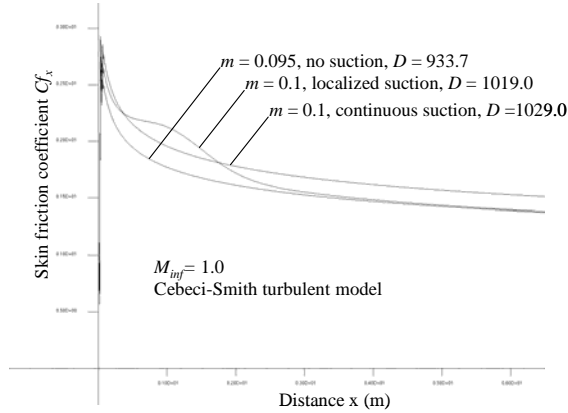

Figure 4. Skin friction coefficient Cf_x against the distance x for various values of the parameter m, $M_\infty = 1.0$ for the case of a cooled wall and application of suction (C-S turbulent model).
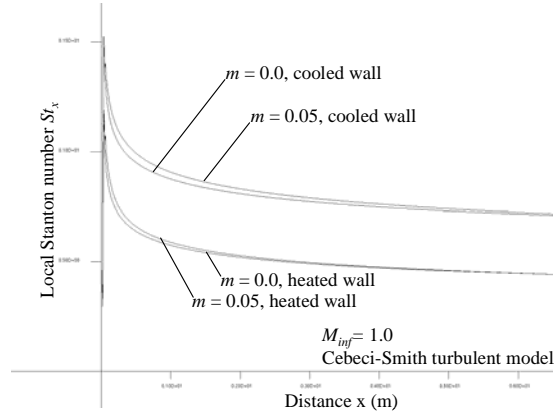
Figure 5. Local Stanton number (St_x) for heated and cooled walls and different values of the dimensionless pressure parameter m (C-S turbulent model).

6 CONCLUSIONS

- A mathematical formulation for the turbulent compressible boundary layer over a wedge was presented.
- Different values of the dimensionless pressure parameter m were examined. When m increases, the dimensionless skin friction coefficient Cf_x and the total drag D increase.
- An instant separation of the turbulent compressible boundary layer over the wedge occurs when $m \geq 0.1$.
- Application of suction retains the boundary layer for larger values of the dimensionless pressure parameter m. Localized suction are more desirable due to smaller total drag D.

References

[1] Falkner, V.M., Skan, S.W., (1931), "Some approximate solutions of the boundary layer equations", Philos. Mag. Vol. 12, No. 80, pp. 865–896.

[2] Kuo Bor-Lih (2005), "Heat transfer analysis for the Falkner–Skan wedge flow by the differential transformation method", International Journal of Heat and Mass Transfer, Vol. 48, pp.5036–5046.

[3] Cheng, W.T., Lin, H.T., (2002), "Non-similarity solution and correlation of transient heat transfer in laminar boundary layer flow over a wedge", International Journal of Engineering Science, Vol. 40, pp. 531–548.

[4] Pantokratoras, A., (2006), "The Falkner–Skan flow with constant wall temperature and variable viscosity" International Journal of Thermal Sciences, Vol. 45, pp. 378–389.

[5] Devi, S.P.A., Kandasamy, R., (2003), "Thermal stratification effects on non linear MHD laminar boundary-layer flow over a wedge with suction or injection", Int. Comm. Heat Mass Transfer, Vol. 30, No. 5, pp. 717-725.

[6] Arnal, D., (1995), "Control of Laminar-Turbulent Transition for Skin Friction Drag Reduction", *in: Control of Flow Instabilities and Unsteady Flows, CISM Course, September 18-22,* pp. 119-153.

[7]   Roy, S., (2000), "Nonuniform slot injection (suction) into a compressible flow", Acta Mechanica, Vol. 139, pp. 43-56.

[8]   Xenos, M., Kafoussias N. and Karahalios, G., (2001), "Magnetohydrodynamic compressible laminar boundary layer adiabatic flow with adverse pressure gradient and continuous or localized mass transfer", Canadian Journal of Physics, Vol. 79, pp. 1247-1263.

[9]   Gad-el-Hak, M. and Bushnell, D.M., (1991), "Status and Outlook of Flow Separation Control", AIAA Paper 91-0037.

[10]   Cebeci, T. and Bradshaw, P., (1984), *Physical and Computational Aspects of Convective Heat Transfer*, Springer-Verlag, New York.

[11]   Kafoussias, N.G. and Xenos, M.A., (2000), "Numerical investigation of two-dimensional turbulent boundary-layer compressible flow with adverse pressure gradient and heat and mass transfer", Acta Mechanica, Vol. 141, pp. 201-223.

[12]   Kafoussias, N.G.and Nanousis, N.D., (1997), "Magnetohydrodynamic laminar boundary-layer flow over a wedge with suction or injection", Canadian Journal of Physics, Vol. 75, pp.733-745.

[13]   Schlichting, H., (1979), *Boundary-Layer Theory*, Trans. by Kestin J., 7th Ed., McGraw-Hill, Inc. New York.

[14]   Cebeci, T.and Smith, A.M.O., (1974), *Analysis of turbulent boundary layers*, Academic Press, New York, pp. 329-370, 258-296.

[15]   Bradshaw, P. (ed.), (1976), Turbulence, *Topics in Applied Physics*, Springer-Verlag, Berlin, 12, pp. 193-195.

[16]   Henkes, R.A.W.M., (1998), "Scaling of equilibrium boundary layers under adverse pressure gradient using turbulent models", AIAA Journal, Vol. 36, No. 3, pp. 320-326.

[17]   Baldwin, B. and Lomax, H. (1978), "Thin–layer aproximation and algebric model for separated turbulent flows", AIAA Paper, pp. 78-205.

[18]   Steger, J.L., (1977) "Impicit finite difference simulation of flow about arbitrary geometries with application to airfoils", AIAA Paper 77-665, presented at AIAA 12th Thermophysics Conference at Albuqurque, New Mex., June 27-29,.

[19]   Pulliam, T.H. and Steger, J.L., (1980), "Impicit Finite-Difference Simulations of Three-Dimensional Compressible Flow", AIAA Journal, Vol.18, No. 2, pp. 159-167.

[20]   Tam, C.J., Orkwis, P.D., (1995), "Comparison of Baldwin–Lomax turbulence models for two–dimensional open cavity computations", AIAA Journal, Vol. 34, No. 3, pp. 629-631.

[21]   Weigand, B., Ferguson, J.R., Crawford, M.E., (1997), "An extended Kays and Crawford turbulent Prandtl number model", International Journal of Heat Mass Transfer, Vol. 40, No. 17, pp. 4191-4196.

[22]   Kafoussias, N., Karabis, A. and Xenos, M., (1999), "Numerical study of two dimensional laminar boundary layer compressible flow with pressure gradient and heat and mass transfer", International Journal of Engineering Science, Vol. 37, pp. 1795-1812.

[23]   Keller, H.B., (1970), A new difference scheme for parabolic problems. *Numerical Solutions of Partial Differetial Equations*, II, J. Bramble (ed.). Academic Press, New York.

[24]   Tannehill, J.C., Anderson, D.A., Pletcher, R.H., (1997), *Computational fluid mechanics and heat transfer*, 2*nd* Edition, Taylor & Francis.

[25]   Davidson, J.H., Kulacki, F.A., Dunn, P.F., (1987) Convective Heat Transfer with Electric and Magnetic Fields, in: S. Kakac, R.K. Shah, W. Aung, *Handbook of single–phase convective heat transfer*, John Wiley & Sons, New York, , pp. 9.1-9.49.

[26]   Cecilio, W.A., Cordeiro, C.J., Milleo, I.S., Santiago, C.D., Zanardini, R.A.D., Yuan, J.Y., (2002), "A note on polynomial interpolation", International Journal of Computer Mathematics, Vol. 79, No. 4, pp. 465-471.

[27]   Xenos, M., Dimas, S. and Kafoussias, N., (2005), "MHD compressible turbulent boundary layer flow with adverse pressure gradient", Acta Mechanica, Vol. 177, No. 1-4, pp. 171-190,

[28]   Wright, R.S. Jr., Sweet, M.R., (1999), *OpenGL SuperBible*, 2*nd* Edition, Waite Group Press.